Supporting Information

N-Type Doping of Fullerene for Planar Perovskite Solar Cells

Qing-Qing Ye, Zhao-Kui Wang, Meng Li, Cong-Cong Zhang, Ke-Hao Hu, and Liang-Sheng Liao*

Jiangsu Key Laboratory for Carbon-Based Functional Materials & Devices, Institute of Functional Nano & Soft Materials (FUNSOM), Soochow University, Suzhou, Jiangsu 215123, China

*Address correspondence to zkwang@suda.edu.cn (Z. K. Wang)

Table of Contents

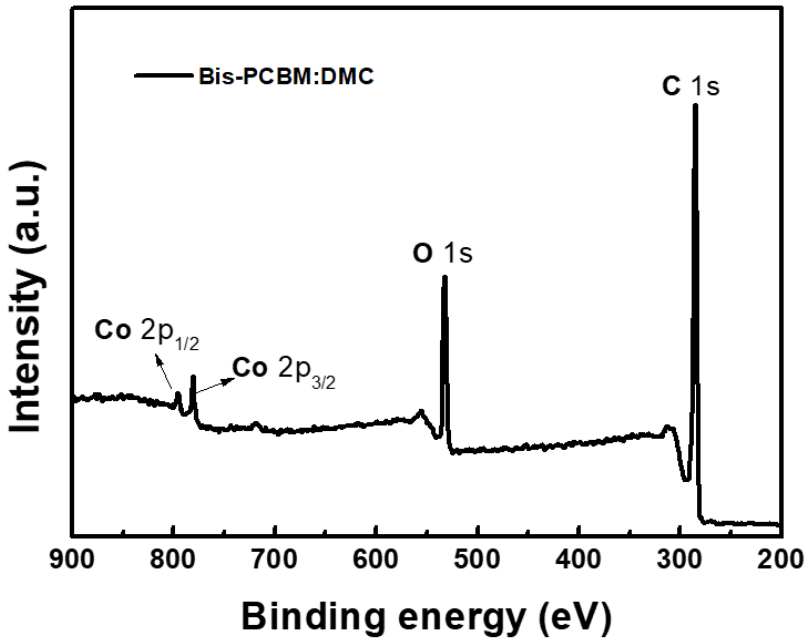

Figure S1. A full scan of XPS spectrum of Bis-PCBM:DMC (0.1 wt%) film on TiO_2.

N-doping of Bis-PCBM by DMC

Figure S2a shows the XPS core-level spectra of Co 2p1/2 and 2p3/2 in pristine DMC and Bis-PCBM: DMC (0.1 wt%) composite films. Compared with pristine DMC sample, the Co 2p peaks in DMC-doped Bis-PCBM film shifted toward higher binding energies from 795.23 to 795.58 eV and from 780.38 to 795.63 eV for Co 2p1/2 and Co 2p3/2, respectively. Figure S2b and S2c presents the O 1s core level in pristine Bis-PCBM and DMC-doped Bis-PCBM films. For pristine Bis-PCBM film, the O 1s peak can be deconvoluted to two peaks locating at 533.38 eV (ascribed to the ionization of 1s electrons from the the single bond oxygen (C–O–C) of the Bis-PCBM side-chain) and 532.18 eV (assigned to ionization of the 1s state of double bonded oxygen (O=C)).[1] In contrast, it can be deconvoluted to three peaks for DMC-doped Bis-PCBM film. The appearance of additional peak located at 530.88 eV is associated with DMC doping, which may cause an environmental change around a portion of the oxygen atoms. In comparison, O 1s in the doped film was observed to shift toward lower binding energies relative to pristine Bis-PCBM film. These opposite shifts of Co 2p and O 1s peaks suggest the occurrence of electron transfer from DMC to Bis-PCBM.

Fourier-transform infrared (FTIR) spectroscopy and Raman spectroscopy are powerful techniques for studying the structural characterization of materials. Figure S2d shows the transmission modes of FTIR spectra of Bis-PCBM, DMC and Bis-PCBM: DMC (0.1 wt%). The peaks around 1604, 1475, 1446, and 1380 cm^{-1}, which are associated with the C=C stretching vibration of aromatic ring, are observed in all three films. Compared to the pristine Bis-PCBM and DMC films, additional peak located at 1319 cm^{-1} which is assigned to the swing outside the surface vibration of CH_3, is observed in DMC-doped Bis-PCBM film.[2] In addition, the peak of 1735 cm^{-1} corresponding to carbonyl stretching vibration of the ester in Bis-PCBM film shifts to 1731 cm^{-1} after DMC doping. The low frequency shift of ester carbonyl stretching vibration is ascribed to a change of π electron distribution in the doped system. This indicates that DMC incorporation could cause partial structural change of Bis-

PCBM. The Raman spectra of Bis-PCBM, DMC and Bis-PCBM: DMC (0.1 wt%) films are presented in Figure S2e. It is found that DMC-doped Bis-PCBM film demonstrated similar characteristic Raman vibration frequency with pristine Bis-PCBM film. However, the doped film is accompanying with a peak positon shift from 966.7cm^{-1} shifted to 977.5cm^{-1} in the direction of larger wavenumber. The shift is ascribed to the charge transfer between Bis-PCBM and DMC owing to the coupling of molecule and electron vibrations.[3] The n-type doping of Bis-PCBM by DMC is further verified by electron spin resonance (ESR) as shown in Figure S2f. Except for the signals generated at the magnetic field about 318.36 and 318.90 mT, pristine Bis-PCBM displays no other obvious radical signals in the ESR spcetra. In contrast, DMC-doped Bis-PCBM film presents a strong signal with g (spectral splitting factor) value of 2.005, which is an obvious evidence of efficient electron transfer from the n-dopant DMC to Bis-PCBM.

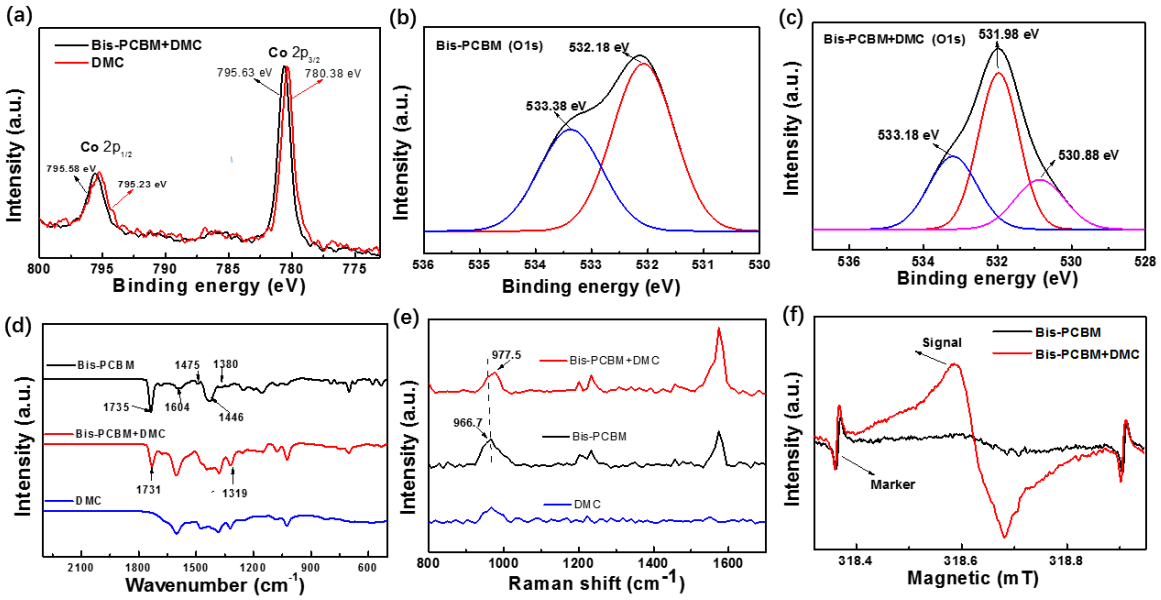

Figure S2. XPS core-level spectra of (a) Co 2p in pristine DMC and Bis-PCBM:DMC films, (b) O 1s in Bis-PCBM film and (c) O 1s in Bis-PCBM:DMC film. (d) FTIR and (e) Raman spectra of pristine DMC, pristine Bis-PCBM and composite Bis-PCBM:DMC films. (f) ESR spectra of pristine Bis-PCBM and composite Bis-PCBM:DMC films.

(1) Brumboiu, I. E.; Ericsson, L.; Hansson, R.; Moons, E.; Eriksson, O.; Brena, B. The influence of oxygen adsorption on the NEXAFS and core-level XPS spectra of the C60 derivative PCBM. *J. Chem. Phys*. **2015**, *142*, 054306.

(2) Kim, B.; Yeom, H. R.; Choi, W. Y.; Jin, Y. K.; Yang, C. Synthesis and characterization of a bis-methanofullerene-4-nitro-cyanostilbene dyad as a potential acceptor for high-performance polymer solar cells. *Tetrahedron* **2012**, *68*, 6696-6700.

(3) Huang, Y. C.; Liao, Y. C.; Li, S. S.; Wu, M. C.; Chen, C. W.; Su, W. F. Study of the effect of annealing process on the performance of p3ht/pcbm photovoltaic devices using scanning-probe microscopy. *Sol. Energ. Mat. SOL. C.* **2009**,*93*, 888-892.

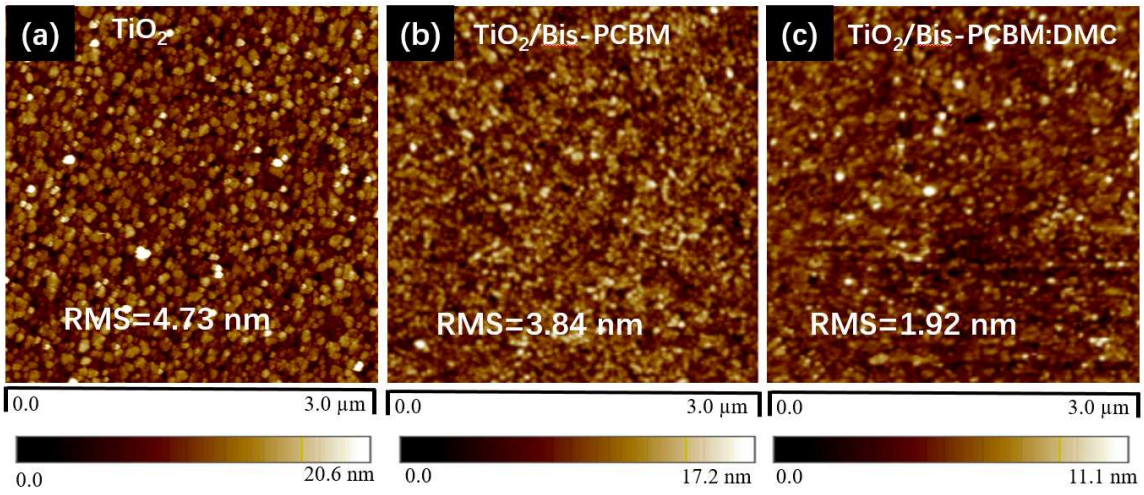

Figure S3. AFM surface images of (a) TiO_2, (b) TiO_2/Bis-PCBM and (c) TiO_2/Bis-PCBM:DMC (0.1 wt%) films.

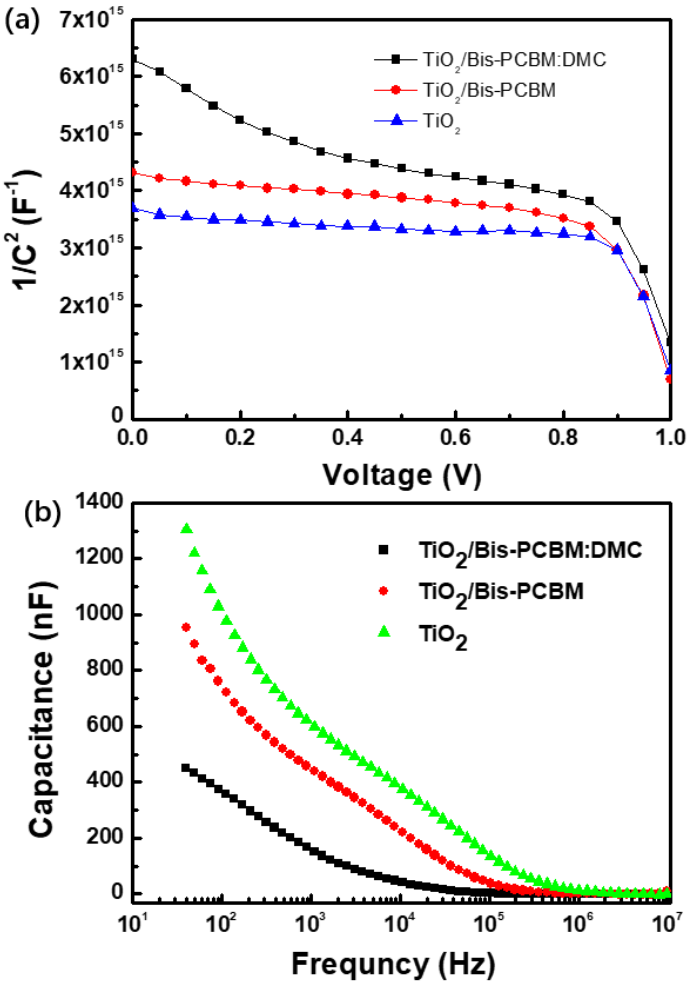

Figure S4. (a) $1/C^2$ versus applied voltage in TiO_2, TiO_2/Bis-PCBM and TiO_2/Bis-PCBM:DMC (0.1 wt%) based perovskite solar cells. (b) Capacitance versus frequency in TiO_2, TiO_2/Bis-PCBM and TiO_2/Bis-PCBM:DMC (0.1 wt%) based perovskite solar cells.

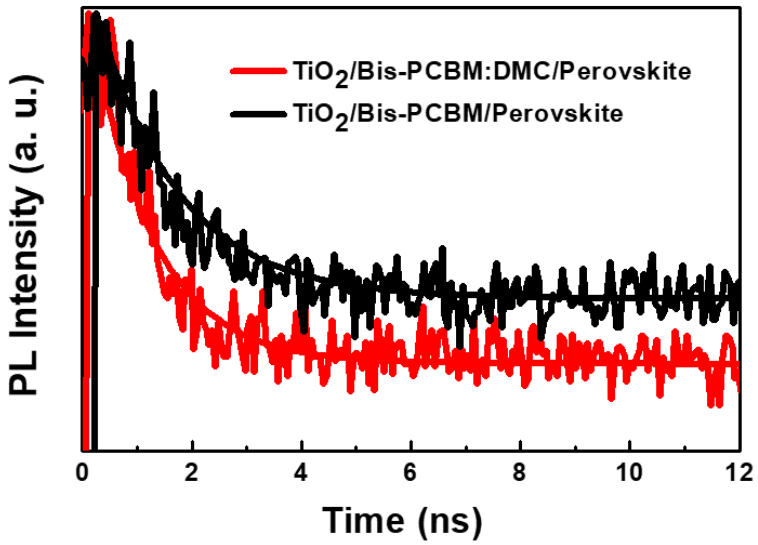

Figure S5. Time-resolved PL spectra of $CH_3NH_3PbI_3$ perovskite films deposited on TiO_2/Bis-PCBM and TiO_2/Bis-PCBM:DMC (0.1 wt%) underlayers.

Table S1. Cell parameters of n-i-p PSCs scanned with forward and reverse directions.

ETLs	V_{OC} (V)	J_{SC} (mA/cm^2)	FF	PCE (%)
TiO_2/Bis-PCBM (reverse)	1.06	22.24	0.74	17.50
TiO_2/Bis-PCBM (forward)	1.01	22.08	0.72	16.32
TiO_2/Bis-PCBM:DMC (reverse)	1.08	23.45	0.78	19.63
TiO_2/Bis-PCBM:DMC (forward)	1.08	23.38	0.75	19.01

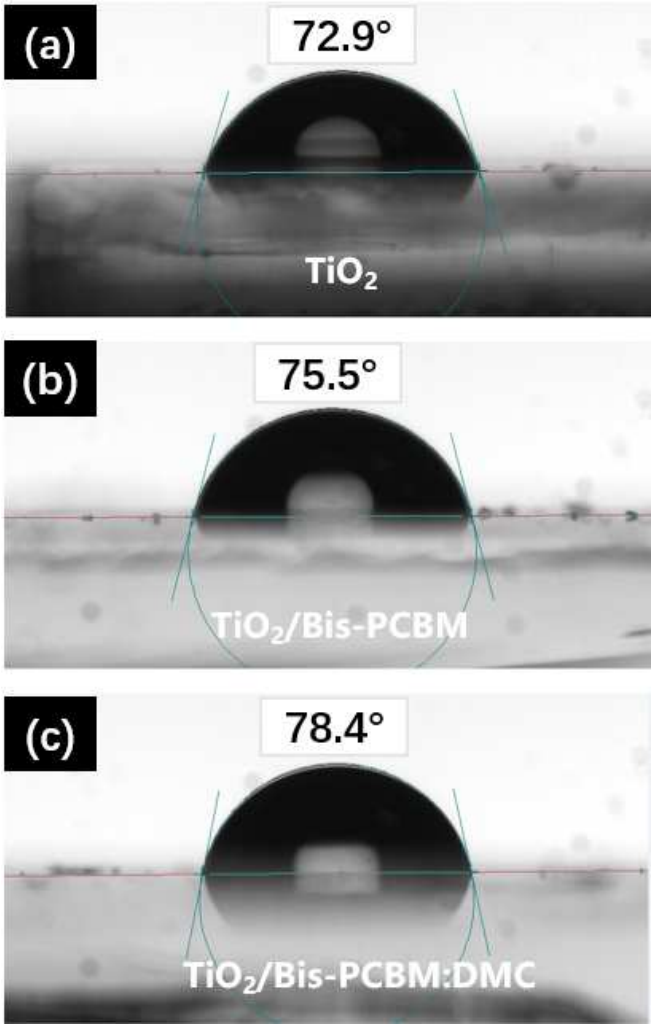

Figure S6. Water contact angles of (a) TiO_2, (b) TiO_2/Bis-PCBM and (c) TiO_2/Bis-PCBM:DMC (0.1 wt%) films.

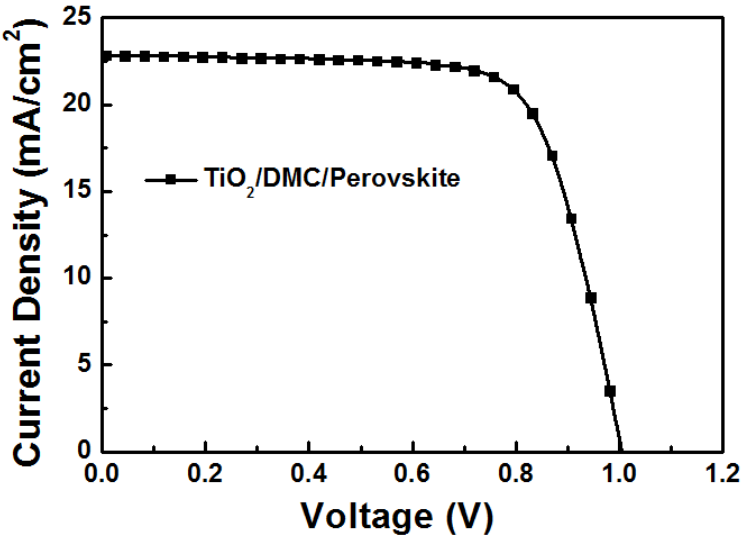

Figure S7. *J-V* curves of the PSC using TiO_2/DMC as the ETL measured under simulated AM 1.5 sunlight of l00 mW/cm^2 irradiance.

Table S2. Cell parameters of PSC using TiO_2/DMC as the ETL.

ETL	V_{OC} (V)	J_{SC} (mA/cm^2)	FF	PCE (%)
TiO_2/DMC/Perovskite	1.01	22.85	0.71	16.58

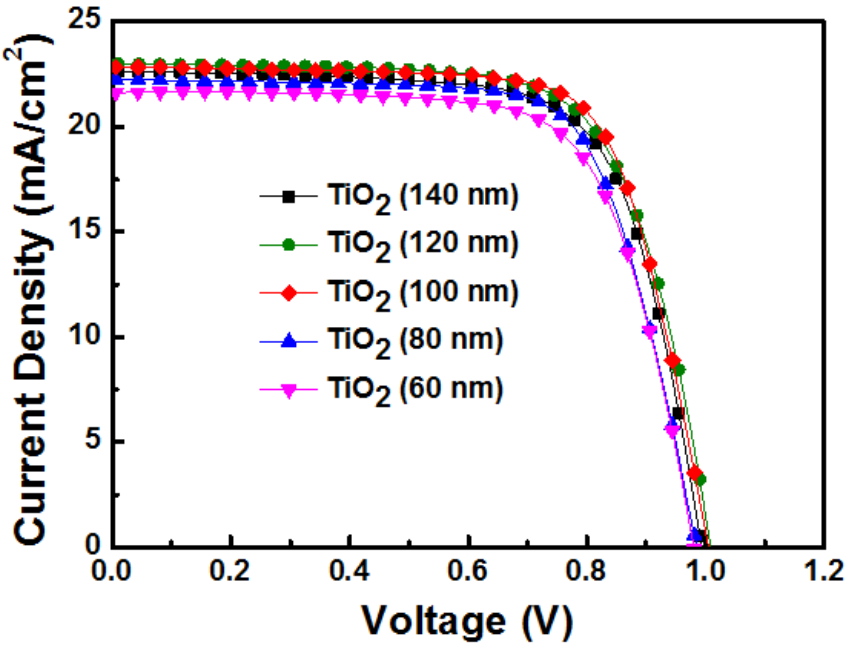

Figure S8. *J-V* curves of the PSC using TiO_2 of different thickness as the ETL .

Table S3. Cell parameters of PSC using TiO_2 of different thickness as the ETL.

ETLs	V_{OC} (V)	J_{SC} (mA/cm^2)	FF	PCE (%)
TiO_2 (140 nm)	0.99	22.64	0.69	15.82
TiO_2 (120 nm)	1.01	22.87	0.69	16.24
TiO_2 (100 nm)	1.01	22.85	0.71	16.58
TiO_2 (80 nm)	0.99	22.25	0.70	15.55
TiO_2 (60 nm)	0.98	21.62	0.70	14.88